Received August 13, 2019, accepted August 21, 2019, date of publication August 23, 2019, date of current version September 6, 2019.

*Digital Object Identifier 10.1109/ACCESS.2019.2937124*

# A Novel Synthetic CT Generation Method Using Multitask Maximum Entropy Clustering

**YIZHANG JIANG[1,2,3], (Member, IEEE), JIAMIN ZHENG[1,2], XIAOQING GU[4], JING XUE[5], AND PENGJIANG QIAN[1,2,3], (Member, IEEE)**
[1]School of Digital Media, Jiangnan University, Wuxi 214122, China
[2]Jiangsu Key Laboratory of Media Design and Software Technology, Wuxi 214122, China
[3]Jiangsu Jiangda Smart Science and Technology Ltd., Jiangsu 214500, China
[4]School of Information Science and Engineering, Changzhou University, Changzhou 213164, China
[5]Department of Nephrology, The Affiliated Wuxi People's Hospital of Nanjing Medical University, Wuxi 214023, China

Corresponding authors: Yizhang Jiang (yzjiang@jiangnan.edu.cn), Jing Xue (475809491@qq.com), and Pengjiang Qian (qianpjiang@jiangnan.edu.cn)

This work was supported in part by the National Natural Science Foundation of China under Grant 61702225 and Grant 61772241, in part by the Natural Science Foundation of Jiangsu Province under Grant BK20160187, in part by the 2018 Six Talent Peaks Project of Jiangsu Province under Grant XYDXX-127, in part by the Science and Technology Demonstration Project for Social Development of Wuxi under Grant WX18IVJN002, in part by the Youth Foundation of the Commission of Health and Family Planning of Wuxi under Grant Q201654, and in part by the Jiangsu Committee of Health under Grant H2018071.

**ABSTRACT** Due to the risk of radiation from computed tomography (CT) scanning on the human body, the number of CT scans that can be performed on an individual each year is limited. However, CT images play a very important role in medical diagnosis. Therefore, this study proposes a method of generating synthetic CT to solve this problem. Considering that magnetic resonance imaging (MRI) is not harmful to the human body, there is no limit on the number of scans that can be performed with this procedure. In this paper, an image segmentation method is used to segment an MRI, and each segment is given a corresponding Hounsfield Unit (HU) value to finally generate a synthetic CT image. Since the image segmentation performance directly affects the generated synthetic CT image, this paper introduces a multitask learning strategy into a maximum entropy clustering (MEC) algorithm. A multitask maximum entropy clustering (MT-MEC) algorithm is proposed, which is used to effectively segment the MRI of the brain. The algorithm can use knowledge from multiple tasks to improve the learning ability of all tasks, and the MEC algorithm can effectively avoid interference from noise. The experimental results show that the proposed MT-MEC algorithm has good image segmentation performance, which results in reliable performance of the final synthetic CT image.

**INDEX TERMS** Synthetic CT, brain MRI, multitask learning, MEC algorithm.

## I. INTRODUCTION

It is well known that CT scanning poses a radiation hazard to the human body. The number of CT scans an individual can receive each year is limited. Too many scans can result in radiation-based harm to the human body. The risk of CT-based damage to the brain—the most important organ in the body—is even greater. Many patients with brain diseases are anxious about obtaining CT scans, which can be an inconvenience for their doctors. Faced with such a scenario, some scholars have proposed a method for automatically generating synthetic CT images [1]–[4]. During acquisition, so it can be used as the basis for synthetic CT imaging. The MRI can be segmented using an image segmentation method, and each segment can be assigned to a corresponding HU value [5], resulting in the generation of a synthetic CT image. The synthetic CT generation schematic is shown below

As seen from the schematic shown in **FIGURE 1**, image segmentation performance directly affects the generation of the synthetic CT. Therefore, it is important to perform the image segmentation steps correctly Image segmentation refers to dividing an image into a series of regions that do not overlap each other. It is a key step in achieving image understanding from image processing to image analysis. Commonly used image segmentation algorithms mainly include fuzzy clustering algorithms [6], [7], multiview

The associate editor coordinating the review of this article and approving it for publication was Yongtao Hao.

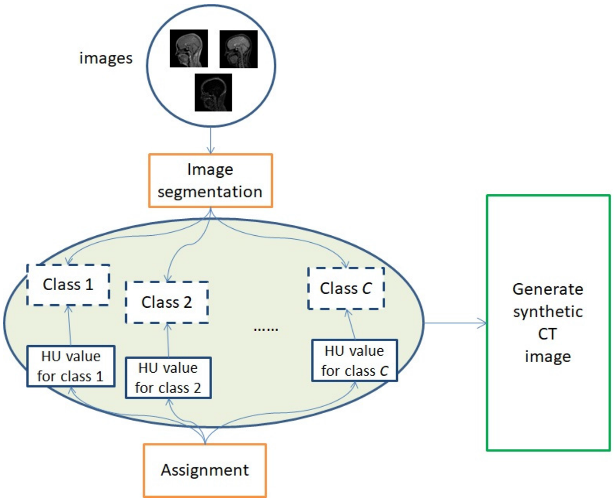


**FIGURE 1.** Synthetic CT generation schematic.

clustering algorithms [8], [9], multitask clustering algorithms [10], [11], transfer clustering algorithms [12], collaborative clustering algorithms [13], neural networks [14] and other types of algorithms [15]–[17].

MRI has many advantages over other imaging techniques. First, MRI has a good imaging effect, clearly reflecting the anatomy of the tissues of organs and the structures of lesions. Second, it is able to obtain an image of each section, unlike other techniques. Finally, it is harmless to the body. These benefits have given the MRI an important role in medicine, so this article chooses to segment the MRI of the brain.

At present, there are many image segmentation algorithms for brain MRIs. According to their different theoretical foundations, they can be divided into the following categories: active contours and level sets, overview classification based on pixel statistical properties, map-based methods, and clustering algorithms. Among them, the clustering algorithm is the most widely used, and its advantages are very obvious: it is simple, efficient, and does not need to be processed by humans. Commonly used clustering algorithms include k-means [18], fuzzy C-means (FCM) [19], MEC [20], probability clustering (PCM) [21], [22] and related, improved algorithms. Prakash et al. proposed a fully automatic brain MRI segmentation algorithm based on FCM, which can effectively overcome the problem of noise sensitivity and image nonuniformity, but the clustering performance of the algorithm is not much improved compared with FCM alone [23]. Deng et al. proposed an improved FCM algorithm for brain MRI segmentation and bias field correction, which improved the robustness of the algorithm to noise, but the running time of the algorithm increased [24]. Ahmed *et al.* improved the objective function of the FCM algorithm to compensate for the defect of MRI intensity nonuniformity [25]. Hanuman *et al.* applied an improved fuzzy entropy clustering (IFEC) algorithm to brain MRIs. This algorithm can process noisy data well, but it does not consider local spatial information [26]. Because the MEC algorithm is more anti-noise than other algorithms, this paper chooses the MEC algorithm as the basis to achieve effective segmentation of brain MRIs. Based on the traditional MEC algorithm, this paper introduces a multitask learning strategy and proposes an MT-MEC algorithm. The experimental results show that the MT-MEC algorithm is robust to noise, and the introduction of a multitask learning strategy takes into account the association between tasks, which improves the clustering performance of the algorithm and greatly improves the segmentation accuracy of the image.

The main work of this study is summarized as follows:

(1) A method for generating a synthetic CT is proposed, which can help obtain CT images without performing a CT scan, resulting in a promising synthetic CT effect.

(2) An image segmentation method for automatically segmenting a brain MRI is proposed. This method introduces a multitask learning strategy. In the simultaneous learning of multiple tasks, the correlation between multiple tasks is used to obtain the common properties of each task to avoid underlearning by the learning machine and improve the generalization performance of individual learning tasks.

(3) Multitask maximum entropy clustering is applied to the brain MRI segmentation to not only improve the segmentation performance of the image but also enhance the effect of the synthetic CT.

The symbols used in the algorithm of this study are described in the following table:

**TABLE 1.** Symbol description.

| Symbol | description |
|---|---|
| $N$ | Total number of samples |
| $C$ | Number of clusters |
| $\mathbf{x}_i$ | $i^{th}$ sample |
| $\mathbf{V}$ | Cluster center matrix; $v_j$ represents the $j^{th}$ cluster center |
| $\mathbf{U}$ | Membership degree matrix; $u_{ij}$ represents the degree to which sample $x_i$ belongs to $v_j$ |
| $\gamma$ | Regular parameter |
| $K$ | Total number of tasks |
| $C_k$ | Number of clusters for the $k^{th}$ task |
| $\mathbf{V}_k$ | Private cluster center matrix of the $k^{th}$ task |
| $N_k$ | Number of samples for the $k^{th}$ task |
| $\mathbf{u}_{ij,k}$ | The degree to which sample $x_i$ belongs to center $v_j$ in the $k^{th}$ task |
| $\mathbf{x}_{i,k}$ | Sample $x_i$ in the $k^{th}$ task |
| $\mathbf{v}_{j,k}$ | Cluster center $v_j$ in the $k^{th}$ task |
| $\lambda$ | Balance parameter to control the influence of the public clustering term |
| $P$ | Number of public cluster centers |
| $\mathbf{o}_p$ | the $p^{th}$ public cluster center |
| $\gamma_1$ | A regularization parameter |
| $\gamma_2$ | A regularization parameter |
| $\mathbf{r}_{jp,k}$ | Membership degree of the $j^{th}$ private cluster center of the $k^{th}$ task belonging to the public clustering center $\mathbf{o}_p$ |

## II. RELATED WORK

### A. MAXIMUM ENTROPY CLUSTERING ALGORITHM

The MEC algorithm reconstructs the objective function of the FCM with a unique entropy concept and obtains a fuzzy clustering algorithm based on the maximum entropy meaning. The concrete expression of the classic MEC algorithm is as follows. The sample set $X = \{x_i \,|x_i \in R^d, i = 1, 2, \ldots, N\}$ is clustered into $C(2 \le C < N)$ subclasses according to a similarity measure. The objective function of the algorithm is as follows:

$$J(U, V) = \sum_{j=1}^{C}\sum_{i=1}^{N} u_{ij}\left\|x_i - v_j\right\|^2 + \gamma\sum_{j=1}^{C}\sum_{i=1}^{N} u_{ij}\ln u_{ij} \quad (1)$$

The constraints that each item in Eq. (1) need to satisfy are as follows

$$\begin{cases} u_{ij} \in [0, 1], & 1 \le j \le C,\ 1 \le i \le N \\ \sum_{j=1}^{C} u_{ij} = 1, & 1 \le i \le N \\ 0 < \sum_{i=1}^{N} u_{ij} < N \end{cases}$$

where $\|\bullet\|$ in Eq. (1) represents the Euclidean distance. Using the Lagrange multiplier method to solve Eq. (1), the expressions of the cluster center and membership degree are as follows:

$$v_j = \frac{\sum_{i=1}^{N} u_{ij} x_i}{\sum_{i=1}^{N} u_{ij}} \quad (2)$$

$$u_{ij} = \frac{\exp\left(-\left\|x_i - v_j\right\|^2/\gamma\right)}{\sum_{h=1}^{C}\exp\left(-\left\|x_i - v_h\right\|^2/\gamma\right)} \quad (3)$$

The traditional MEC algorithm usually deals with single task data. When processing multitask data, the algorithm uses the same steps as the single task data to process multitask data, which greatly affects the performance of the MEC algorithm. **FIGURE 2** shows the principal diagram explaining the clustering of multitask data by the MEC algorithm.

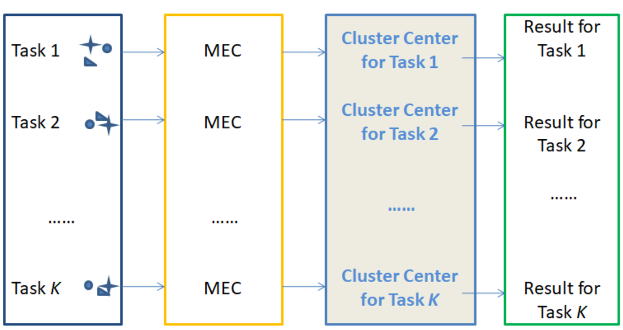


**FIGURE 2. Schematic diagram of MEC algorithm for processing multitask data.**

### B. MULTITASK LEARNING STRATEGY

Machine learning algorithms that learn multiple tasks at the same time use multitask learning to improve traditional single task learning performance [27]. In the process of learning multiple tasks at the same time, the correlation between multiple tasks is used to obtain common properties of each task to avoid underlearning by the learning machine and improve the generalization performance of the individual learning tasks. **FIGURE 3** shows the multitask learning model.

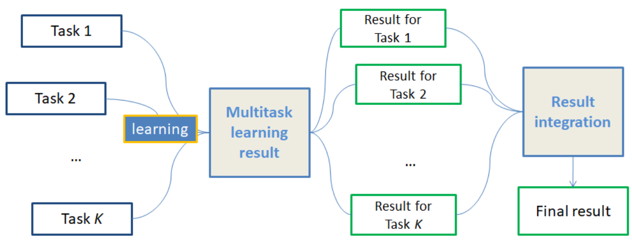


**FIGURE 3. Model of multitask learning.**

As seen from the above figure, multitask learning is a method of transfer learning [28], which can use the meaningful commonality of other related tasks to improve the performance of the entire learning task. Multitask learning has many advantages over traditional machine learning. In terms of cluster analysis, Jacob *et al.* [29] proposed a multitask learning clustering algorithm by assuming that each task is clustered by group and that the tasks within the same group are similar. Gu and Zhou [30] proposed a shared subspace multitasking clustering analysis algorithm. Zhang and Zhou [31] proposed a multitask clustering algorithm based on domain adaptation [32]. Zhong and Kwok [33] proposed a flexible task-clustered algorithm through the Accelerated proximal method [34]. Xu *et al.* [35] proposed a multitask learning collaborative clustering algorithm with task characteristics. In terms of pattern classification, Evgeniou and Pontil [36] applied a hierarchical Bayesian model [37] to an SVM to propose a multitask learning SVM. Liang *et al.* [38] proposed a multitask enhanced SVM based on an enhanced SVM [39]. Zhu et al. [40] proposed a multitask infinite latent SVM based on an infinite SVM [41]. He *et al.* [42] proposed two types of multitask SVM, MTL-OSVM I and MTL-OSVM II, based on a one-class SVM [43]. Xu *et al.* [44] proposed a multitask least-squares SVM based on a least-squares SVM [45]. Li et al. [46] proposed a multitask proximal SVM based on a proximal SVM [47]. Xie and Sun [48] proposed a multitask centroid twin SVM based on a twin SVM [49].

## III. MULTITASK MAXIMUM ENTROPY CLUSTERING (MT-MEC) ALGORITHM APPLIED TO BRAIN MRI SEGMENTATION

### A. MULTITASK MAXIMUM ENTROPY CLUSTERING ALGORITHM (MT-MEC)

The traditional MEC algorithm is mainly used to cluster single task data sets. For the clustering of multitask data sets, the MEC algorithm is no longer applicable. To solve this problem, this paper introduces a multitask learning strategy into the MEC algorithm, called the MT-MEC algorithm. **FIGURE 4** shows the schematic of the algorithm for processing multitask data.

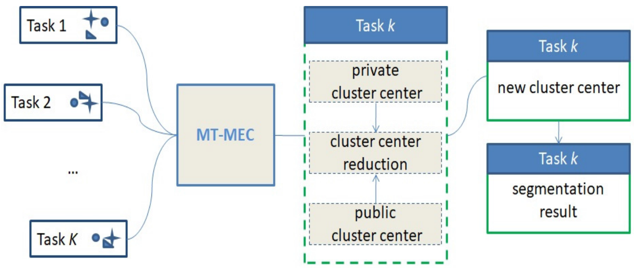


**FIGURE 4. Schematic diagram of clustering multitask data with the MT-MEC algorithm.**

The objective function of the MT-MEC algorithm is as follows:

$$\begin{aligned} \min J(\mathbf{U}, \mathbf{V}, \mathbf{R}, \mathbf{O}) &= \sum_{k=1}^{K}\sum_{j=1}^{C_k}\sum_{i=1}^{N_k} u_{ij,k}\left\|\mathbf{x}_{i,k}-\mathbf{v}_{j,k}\right\|^2 \\ &+ \lambda\sum_{k=1}^{K}\sum_{p=1}^{P}\sum_{j=1}^{C_k} r_{jp,k}\left\|\mathbf{v}_{j,k}-\mathbf{o}_p\right\|^2 \\ &+ \gamma_1\sum_{k=1}^{K}\sum_{j=1}^{C_k}\sum_{i=1}^{N_k} u_{ij,k}\ln u_{ij,k} \\ &+ \gamma_2\sum_{k=1}^{K}\sum_{p=1}^{P}\sum_{j=1}^{C_k} r_{jp,k}\ln r_{jp,k} \\ s.t.\ u_{ij,k}\in[0,1],\ &\sum\nolimits_{j=1}^{C} u_{ij,k}=1,\ \sum\nolimits_{p=1}^{P} r_{jp,k}=1, \\ 1\le i\le N_k,\ &1\le j\le C_k,\ 1\le p\le P,\ 1\le k\le K. \end{aligned} \tag{4}$$

where $\lambda$ is a balance parameter that can be used to adjust the influence of the public clustering term. The optimal value of coefficient $\lambda(\lambda > 0)$ can be obtained using a cross-validation strategy. $r_{jp,k}$ denotes the degree to which $v_{j,k}$ belongs to the public clustering center $\mathbf{o}_p$. The closer $r_{jp,k}$ is to 1, the closer the private class center is to the public class center. The purpose of the $\sum_{k=1}^{K}\sum_{j=1}^{C_k}\sum_{i=1}^{N_k} u_{ij,k}\left\|\mathbf{x}_{i,k}-\mathbf{v}_{j,k}\right\|^2 + \gamma_1\sum_{k=1}^{K}\sum_{j=1}^{C_k}\sum_{i=1}^{N_k} u_{ij,k}\ln u_{ij,k}$ in the above Eq. (4) is to obtain the private class center $\boldsymbol{V}$ of each task. The purpose of the $\lambda\sum_{k=1}^{K}\sum_{p=1}^{P}\sum_{j=1}^{C_k} r_{jp,k}\left\|\mathbf{v}_{j,k}-\mathbf{o}_p\right\|^2 + \gamma_2\sum_{k=1}^{K}\sum_{p=1}^{P}\sum_{j=1}^{C_k} r_{jp,k}\ln r_{jp,k}$ is to obtain the public class center $\boldsymbol{O}$ of $K$ tasks. In this way, the public and private centers of each task can be obtained. The segmentation result of each task is represented by a combination of public and private class centers, namely, $\boldsymbol{V}_k + \boldsymbol{O}$.

To reduce the class center of each task as much as possible and obtain the optimal clustering effect of the multitask data, this paper proposes the following central reduction strategy:

$$\Gamma = \begin{cases} \mathbf{v}_{j,k} \text{ is very close to public } \mathbf{o}_p, & \\ \quad \text{and then delete } \mathbf{v}_{j,k} \text{ from private } \mathbf{V}_k; & \text{if } r_{jp,k} \ge \Theta \\ \mathbf{v}_{j,k} \text{ is far away from public } \mathbf{o}_p, & \\ \quad \text{and then take no operation;} & \text{if } r_{jp,k} < \Theta \end{cases} \tag{5}$$

The algorithm performance is optimal when the threshold $\Theta$ is set to 0.95. $\boldsymbol{V}_k + \boldsymbol{O}$ changes to $\boldsymbol{V}_k^{'} + \boldsymbol{O}$ following the center reduction strategy. To solve Eq. (4), it is converted to the following unconstrained minimization problem

$$\begin{aligned} J(\mathbf{U}, \mathbf{R}, \mathbf{V}, \mathbf{O}) &= \sum_{k=1}^{K}\sum_{j=1}^{C_k}\sum_{i=1}^{N_k} u_{ij,k}\left\|\mathbf{x}_{i,k}-\mathbf{v}_{j,k}\right\|^2 \\ &+ \lambda\sum_{k=1}^{K}\sum_{p=1}^{P}\sum_{j=1}^{C_k} r_{jp,k}\left\|\mathbf{v}_{j,k}-\mathbf{o}_p\right\|^2 \\ &+ \gamma_1\sum_{k=1}^{K}\sum_{j=1}^{C_k}\sum_{i=1}^{N_k} u_{ij,k}\ln u_{ij,k} \\ &+ \gamma_2\sum_{k=1}^{K}\sum_{p=1}^{P}\sum_{j=1}^{C_k} r_{jp,k}\ln r_{jp,k} \\ &+ \sum_{k=1}^{K}\sum_{i=1}^{N_k}\alpha_{i,k}\Big(1-\sum\nolimits_{j=1}^{C} u_{ij,k}\Big) \\ &+ \sum_{k=1}^{K}\sum_{j=1}^{C_k}\beta_{j,k}\Big(1-\sum\nolimits_{p=1}^{P} r_{jp,k}\Big) \end{aligned} \tag{6}$$

The derivative of each variable in Eq. (6) is then set to 0, resulting in the following variable expressions:

$$u_{ij,k} = \exp\left(-\frac{\left\|\mathbf{x}_{i,k}-\mathbf{v}_{j,k}\right\|^2}{\gamma_1}\right)\Bigg/\sum_{l=1}^{C}\left(-\frac{\left\|\mathbf{x}_{i,k}-\mathbf{v}_{l,k}\right\|^2}{\gamma_1}\right) \tag{7}$$

$$\mathbf{v}_{j,k} = \Big(\sum_{i=1}^{N_k} u_{ij,k}\,\mathbf{x}_{i,k} + \lambda\sum_{p=1}^{P} r_{jp,k}\mathbf{o}_p\Big)\Big/\Big(\sum_{i=1}^{N_k} u_{ij,k} + \lambda\sum_{p=1}^{P} r_{jp,k}\Big) \tag{8}$$

$$r_{jp,k} = \exp\left(-\frac{\left\|\mathbf{v}_{j,k}-\mathbf{o}_p\right\|^2}{\gamma_2}\right)\Bigg/\sum_{l=1}^{P}\left(-\frac{\left\|\mathbf{v}_{j,k}-\mathbf{o}_l\right\|^2}{\gamma_2}\right) \tag{9}$$

$$\mathbf{o}_p = \sum_{k=1}^{K}\sum_{j=1}^{C_k} r_{jp,k}\mathbf{v}_{j,k}\Bigg/\sum_{k=1}^{K}\sum_{j=1}^{C_k} r_{jp,k} \tag{10}$$

The execution steps of the MT-MEC algorithm are as follows:

### B. BRAIN MRI DATA SET INTRODUCTION

We adopted a real ultrashort echo time (UTE) and the modified Dixon PET/MR brain image dataset, which was used in our pervious several studies [50]–[52]. This dataset consists

**Algorithm 1** MT-MEC

**Step 1** Set the total number of tasks $K$, the number of private classes $C_k$ for each task, the number of public class centers $p \left(2 \le p \le \sum_{k=1}^{K} C_k\right)$ for all tasks, the precision threshold $\varepsilon$, the maximum number of iterations $T_{max}$, the regular parameters $\gamma_1$ and $\gamma_2$, the threshold of the central reduction strategy $\Theta$, and the balance parameters $\lambda(\lambda > 0)$. Initialize the private class center $\mathbf{v}_{j,k}$ for each task and the public class center $\mathbf{o}_p$ for all tasks;

**Step 2** Iteratively calculate the $\boldsymbol{u}_{ij,k}$ of each task using (7);

**Step 3** Iteratively calculate the $\boldsymbol{v}_{j,k}$ of each task using (8);

**Step 4** Iteratively calculate the $\boldsymbol{r}_{jp,k}$ of each task using (9);

**Step 5** Iteratively calculate $\boldsymbol{o}_p$ using (10);

**Step 6** The iteration terminates when the iteration termination condition is met, otherwise it jumps to step 2 to continue the iteration.

of three different sequences (Dixon-fat, Dixon-water, and $R2^*$) from 9 patients, an example of which is shown in **FIGURE 5**. A detailed introduction to and description of this dataset can be found in our previous studies [50]–[52].


**FIGURE 5.** **The adopted brain images.**

## IV. EXPERIMENTAL STUDY

The segmentation performance of the proposed MT-MEC algorithm will be evaluated in the following sections. The comparison algorithms are the classic FCM and MEC. The data set used in the experiment is the Ultra Short Echo Time (UTE) and modified Dixon PET/MR [50]–[52].

### A. EXPERIMENTAL SETTINGS

The amount of data in medical images can be on the order of millions of data instances. Therefore, in order to improve the applicability of the algorithm, a sample strategy is used in the process of performing the clustering algorithm, that is, the label of the data instance is obtained by the k-nearest neighbor strategy. The sampling strategy used guarantees the consistency of the algorithm and ensures the fairness of random data quality, reporting all results after ten runs of each method under each parameter set. This process judges the robustness of the sampling strategy and the performance of the algorithm.

During the experiment, the parameters of the comparison algorithms FCM and MEC and the proposed MT-MEC are as follows. The fuzzy coefficient $m$ of the FCM algorithm is selected from the set $\{1.1{:}0.1{:}2.5\}$. The parameter $\gamma$ of the MEC is selected from the set $\{10^{-6}, 10^{-5}, \ldots, 10^5, 10^6\}$. The parameters $\lambda$, $\gamma_1$ and $\gamma_2$ of our proposed MT-MEC are all selected from the set $\{10^{-6}, 10^{-5}, \ldots, 10^5, 10^6\}$. All the parameters used in the experiment were determined using a grid search strategy with normalized experimental data.

To verify whether the effect of the synthetic CT is ideal, the contrast image used in this paper is a real brain CT map. The evaluation indexes are the root mean square error (RMSE), the mean absolute prediction deviation (MAPD), and R [53]. Smaller values of RMSE and MAPD and larger values of R indicate better performance of the algorithm. The PC used in the experiment was an Intel Core i5-6200 2.30 GHz CPU with 4 GB RAM, and the simulation was run with MATLAB R2016a (64-bit).

### B. EXPERIMENTAL RESULTS AND DISCUSSION

Table 2 shows the brain MRI segmentation results of nine patients we randomly selected from the data set. The segmentation results are given using the mean and standard deviation values of RMSE, MAPD and R. It can be seen from the results in Table 2 that the segmentation performance of the MT-MEC algorithm is better than the FCM and MEC algorithms. This is because the introduction of a multitask learning strategy makes the algorithm consider the correlation between tasks and improves the clustering performance of the algorithm. It can be inferred from the standard deviation values that the MT-MEC algorithm has good stability, with minimal fluctuations in the results after each operation. After segmenting the brain MRIs using the MT-MEC algorithm, each class of HU values is assigned to generate a synthetic CT image. **FIGURE 6** shows the synthetic CT generated image following MRI segmentation for 9 patients and the corresponding real brain CT image.

Combining the segmentation results given in Table 2 with the results of the synthetic CT given in Figure 6, the following can be analyzed:

1) In terms of image segmentation performance, it can be seen from the values of the three evaluation indicators that the performance of the MT-MEC algorithm is substantially better than that of the FCM and MEC algorithms. The standard deviation values of the MT-MEC algorithm are lower than those of the two comparison algorithms, indicating that the MT-MEC algorithm is robust and insensitive to parameter changes.

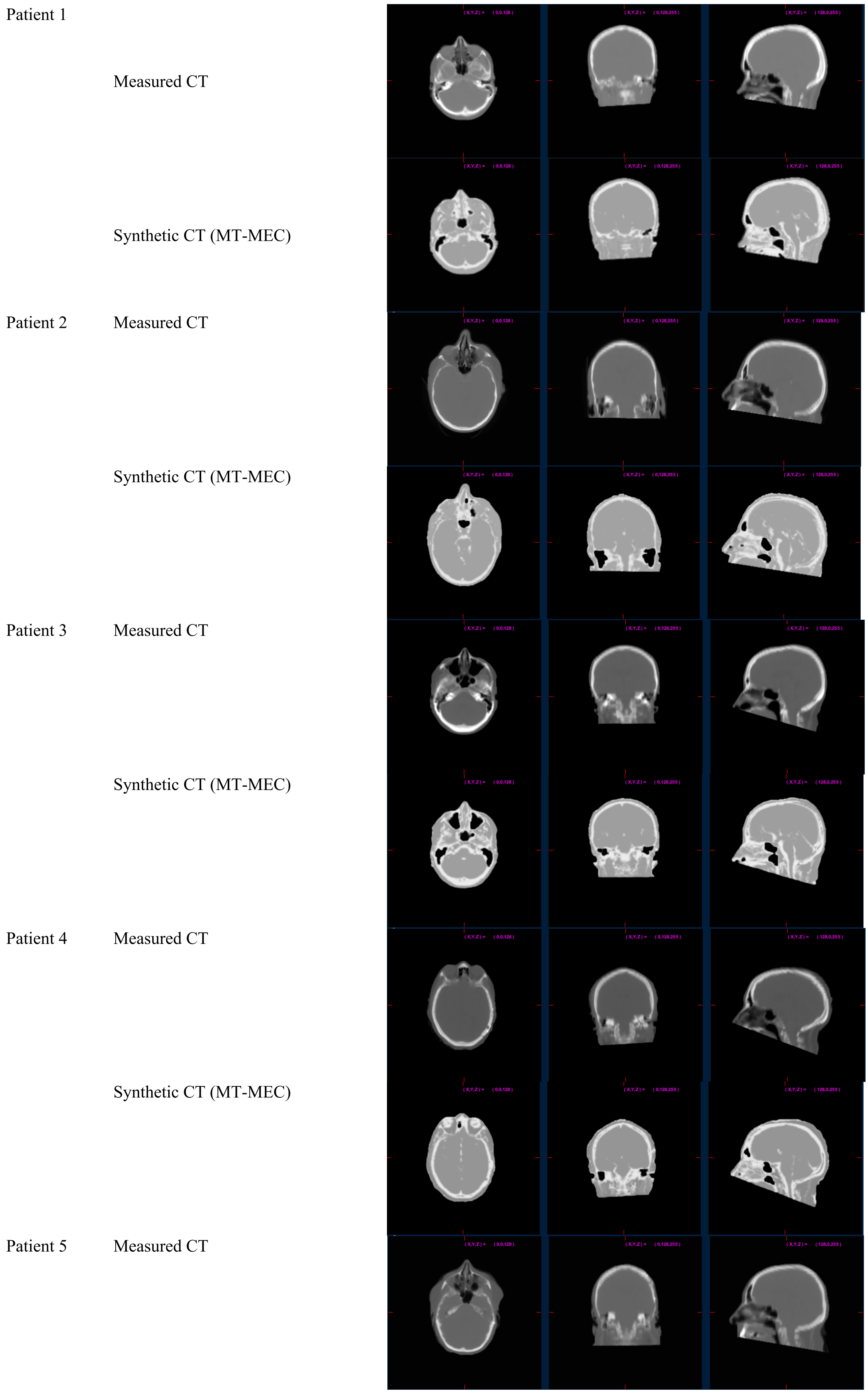


**FIGURE 6. Synthetic CT images generated with our proposed MT-MEC algorithm for Patients 1 to 9.**

Synthetic CT (MT-MEC)

Patient 6 Measured CT

Synthetic CT (MT-MEC)

Patient 7 Measured CT

Synthetic CT (MT-MEC)

Patient 8 Measured CT

Synthetic CT (MT-MEC)

Patient 9 Measured CT

Synthetic CT (MT-MEC)

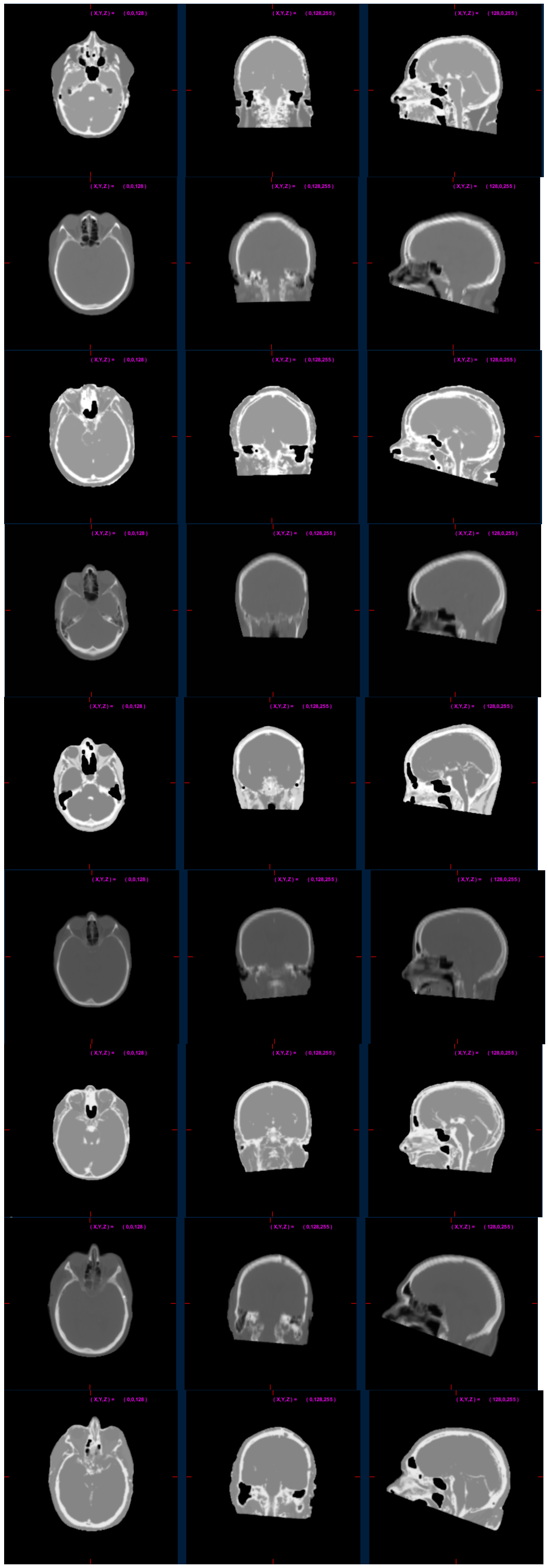

**FIGURE 6.** ***(Continued.)*** **Synthetic CT images generated with our proposed MT-MEC algorithm for Patients 1 to 9.**

**TABLE 2.** Performance comparison of the three clustering algorithms.

| Dataset | | RMSE | | | MAPD | | | R | | |
|---|---|---|---|---|---|---|---|---|---|---|
| | | FCM | MEC | MT-MEC | FCM | MEC | MT-MEC | FCM | MEC | MT-MEC |
| Patient 1 | mean | 201.10 | 270.43 | **171.59** | 110.91 | 166.38 | **105.74** | 0.85 | 0.70 | **0.88** |
| | std | 20.95 | 13.41 | **7.32** | 16.09 | 18.27 | **2.36** | 0.02 | 0.06 | **0.01** |
| Patient 2 | mean | 260.94 | 313.41 | **198.65** | 141.39 | 180.27 | **126.23** | 0.72 | 0.56 | **0.76** |
| | std | 37.51 | 8.95 | **10.72** | 20.20 | 19.20 | **1.89** | 0.07 | 0.06 | **0.00** |
| Patient 3 | mean | 205.26 | **198.01** | 200.43 | 119.89 | **103.45** | 105.26 | 0.82 | **0.84** | 0.82 |
| | std | 26.96 | **9.69** | 5.79 | 15.98 | **16.90** | 4.38 | 0.04 | **0.01** | 0.00 |
| Patient 4 | mean | 232.90 | 308.95 | **226.23** | 137.75 | 193.20 | **132.17** | 0.83 | 0.66 | **0.87** |
| | std | 25.36 | 21.35 | **10.61** | 17.36 | 15.82 | **3.28** | 0.02 | 0.00 | **0.02** |
| Patient 5 | mean | **238.96** | 302.74 | 246.61 | **123.96** | 167.21 | 128.32 | **0.79** | 0.65 | 0.78 |
| | std | **12.38** | 27.43 | 2.57 | **11.41** | 16.38 | 2.90 | **0.01** | 0.00 | 0.00 |
| Patient 6 | mean | 220.55 | 269.69 | **213.31** | 131.70 | 163.90 | **103.68** | 0.77 | 0.61 | **0.81** |
| | std | 11.69 | 28.01 | **8.57** | 4.22 | 16.45 | **8.16** | 0.01 | 0.04 | **0.02** |
| Patient 7 | mean | 194.47 | 283.09 | **190.31** | 109.56 | 170.70 | **100.44** | 0.84 | 0.63 | **0.87** |
| | std | 15.92 | 32.74 | **2.75** | 11.96 | 16.21 | **2.02** | 0.01 | 0.05 | **0.00** |
| Patient 8 | mean | 249.31 | 271.35 | **230.25** | 127.19 | 151.82 | **122.60** | 0.69 | 0.60 | **0.72** |
| | std | 39.38 | 23.09 | **7.17** | 23.23 | 17.70 | **1.72** | 0.09 | 0.03 | **0.01** |
| Patient 9 | mean | 210.490 | 295.82 | **200.51** | 120.23 | 181.30 | **118.83** | 0.87 | 0.73 | **0.88** |
| | std | 17.54 | 25.82 | **6.15** | 12.94 | 18.30 | **2.19** | 0.01 | 0.03 | **0.00** |

2) The synthetic CT image in Figure 6 shows that the MT-MEC algorithm can accurately segment the bone, soft tissue and air in the brain. The segmentation result of the MT-MEC algorithm is more accurate than that of the comparison algorithms.

3) Visual observation of the comparison results in Figure 6 shows that the synthetic CT images of Patients 1-9 are very close to the real images, which fully demonstrates the effectiveness of the synthetic CT generation method in this paper. However, there are still a few cases where the tissue imaging is not clear enough in the synthetic CT image. It is possible that some noise affects the segmentation performance of the MT-MEC algorithm.

## V. CONCLUSION

This study proposes a method of automatically generating a synthetic CT image. The method first performs image segmentation on a brain MRI, assigns HU values to each class, and finally generates a synthetic CT image. The main contribution of this paper is the proposal of the MT-MEC algorithm, which was applied to the segmentation of brain MRIs. Because the proposed MT-MEC algorithm considers the correlation between multiple tasks, and the MEC algorithm has better antinoise performance than other clustering algorithms, the MT-MEC algorithm has good segmentation performance for brain MRIs, which produces accurate, clear CT images. Experiments show that the proposed MT-MEC algorithm has better segmentation performance than the FCM and MEC algorithms, resulting in a very good synthetic CT effect and can serve as a valuable reference for medical diagnosis.

## REFERENCES


[1] S.-H. Hsu, Q. Peng, and W. A. Tomé, "On the generation of synthetic CT for a MRI-only radiation therapy workflow for the abdomen," *J. Phys., Conf. Ser.*, vol. 1154, no. 1, Mar. 2019, Art. no. 012011.

[2] Y. Liu, Y. Lei, Y. Wang, T. Wang, L. Ren, L. Lin, M. McDonald, W. J. Curran, T. Liu, J. Zhou, and X. Yang, "MRI-based treatment planning for proton radiotherapy: Dosimetric validation of a deep learning-based liver synthetic CT generation method," *Phys. Med. Biol.*, vol. 64, no. 14, Jul. 2019, Art. no. 145015.

[3] Y. Lei, J. Harms, T. Wang, S. Tian, J. Zhou, H.-K. Shu, J. Zhong, H. Mao, W. J. Curran, T. Liu, and X. Yang, "MRI-based synthetic CT generation using semantic random forest with iterative refinement," *Phys. Med. Biol.*, vol. 64, no. 8, Apr. 2019, Art. no. 085001.

[4] S. Kazemifar, S. McGuire, R. Timmerman, Z. Wardak, D. Nguyen, Y. Park, S. Jiang, and A. Owrangi, "MRI-only brain radiotherapy: Assessing the dosimetric accuracy of synthetic CT images generated using a deep learning approach," *Radiotherapy Oncol.*, vol. 136, pp. 56–63, Jul. 2019.

[5] W. Schneider, T. Bortfeld, and W. Schlegel, "Correlation between CT numbers and tissue parameters needed for Monte Carlo simulations of clinical dose distributions," *Phys. Med. Biol.*, vol. 5, no. 2, pp. 459–478, Feb. 2000.

[6] P. Qian, Y. Jiang, Z. Deng, L. Hu, S. Sun, S. Wang, and R. F. Muzic, Jr., "Cluster prototypes and fuzzy memberships jointly leveraged cross-domain maximum entropy clustering," *IEEE Trans. Cybern.*, vol. 46, no. 1, pp. 181–193, Jan. 2016.

[7] P. Qian, K. Zhao, Y. Jiang, K.-H. Su, Z. Deng, S. Wang, and R. F. Muzic, Jr., "Knowledge-leveraged transfer fuzzy c-means for texture image segmentation with self-adaptive cluster prototype matching," *Knowl. Based Syst.*, vol. 130, pp. 33–50, Aug. 2017.

[8] P. Qian, J. Zhou, Y. Jiang, F. Liang, K. Zhao, S. Wang, K. Su, and R. Muzic, "Multi-view maximum entropy clustering by jointly leveraging inter-view collaborations and intra-view-weighted attributes," *IEEE Access*, vol. 6, pp. 28594–28610, 2018.

[9] Y. Jiang, Z. Deng, F.-L. Chung, G. Wang, P. Qian, K.-S. Choi, and S. Wang, "Recognition of epileptic EEG signals using a novel multiview TSK fuzzy system," *IEEE Trans. Fuzzy Syst.*, vol. 25, no. 1, pp. 3–20, Feb. 2017.

[10] Y. Jiang, F.-L. Chung, H. Ishibuchi, Z. Deng, and S. Wang, "Multitask TSK fuzzy system modeling by mining intertask common hidden structure," *IEEE Trans. Cybern.*, vol. 45, no. 3, pp. 534–547, Mar. 2015.

[11] Y. Jiang, K. Zhao, K. Xia, J. Xue, L. Zhou, Y. Ding, and P. Qian, "A novel distributed multitask fuzzy clustering algorithm for automatic MR brain image segmentation," *J. Med. Syst.*, vol. 43, no. 5, Mar. 2019, Art. no. 118.

[12] Y. Jiang, D. Wu, Z. Deng, P. Qian, J. Wang, G. Wang, F.-L. Chung, K.-S. Choi, and S. Wang, "Seizure classification from EEG signals using transfer learning, semi-supervised learning and TSK fuzzy system," *IEEE Trans. Neural Syst. Rehabil. Eng.*, vol. 25, no. 12, pp. 2270–2284, Dec. 2017.

[13] Y. Jiang, F.-L. Chung, S. Wang, Z. Deng, J. Wang, and P. Qian, "Collaborative fuzzy clustering from multiple weighted views," *IEEE Trans. Cybern.*, vol. 45, no. 4, pp. 688–701, Apr. 2015.

[14] L. Liu, Y. Ji, Y. Gao, and L. Kuang, "Classification of epileptic electroencephalograms signal based on integrated radius-basis-function neural-network," *J. Med. Imag. Health Inform.*, vol. 8, no. 7, pp. 1462–1467, Sep. 2018.
[15] P. Qian, Y. Jiang, S. Wang, K.-H. Su, J. Wang, L. Hu, and R. F. Muzic, "Affinity and penalty jointly constrained spectral clustering with all-compatibility, flexibility, and robustness," *IEEE Trans. Neural Netw. Learn. Syst.*, vol. 28, no. 5, pp. 1123–1138, May 2017.
[16] K. Xia, H. Yin, P. Qian, Y. Jiang, and S. Wang, "Liver semantic segmentation algorithm based on improved deep adversarial networks in combination of weighted loss function on abdominal CT images," *IEEE Access*, vol. 7, pp. 96349–96358, 2019.
[17] K. Xia, H.-S. Yin, and Y.-D. Zhang, "Deep semantic segmentation of kidney and space-occupying lesion area based on SCNN and ResNet models combined with SIFT-flow algorithm," *J. Med. Syst.*, vol. 43, Nov. 2019, Art. no. 2.
[18] T. Kanungo, D. M. Mount, N. S. Netanyahu, C. D. Piatko, R. Silverman, and A. Y. Wu, "An efficient K-means clustering algorithm: Analysis and implementation," *IEEE Trans. Pattern Anal. Mach. Intell.*, vol. 24, no. 7, pp. 881–892, Jul. 2002.
[19] J. C. Bezdek, *Pattern Recognition with Fuzzy Objective Function Algorithms*. New York, NY, USA: Plenum Press, 1981.
[20] R.-P. Li and M. Mukaidono, "A maximum-entropy approach to fuzzy clustering," in *Proc. 4th IEEE Int. Conf. Fuzzy Syst.*, Yokohama, Japan, Mar. 1995, pp. 2227–2232.
[21] R. Krishnapuram and J. M. Keller, "A possibilistic approach to clustering," *IEEE Trans. Fuzzy Syst.*, vol. 1, no. 2, pp. 98–110, May 1993.
[22] R. Krishnapuram and J. M. Keller, "The possibilistic C-means algorithm: Insights and recommendations," *IEEE Trans. Fuzzy Syst.*, vol. 4, no. 3, pp. 385–393, Aug. 1996.
[23] R. M. Prakash and R. S. S. Kumari, "Fuzzy C means integrated with spatial information and contrast enhancement for segmentation of MR brain images," *Int. J. Imag. Syst. Technol.*, vol. 26, no. 2, pp. 116–123, 2016.
[24] W.-Q. Deng, X.-M. Li, X. Gao, and C.-M. Zhang, "A modified fuzzy C-means algorithm for brain MR image segmentation and bias field correction," *J. Comput. Sci. Technol.*, vol. 31, no. 3, pp. 501–511, May 2016.
[25] M. N. Ahmed, S. M. Yamany, N. Mohamed, A. Farag, and T. Moriarty, "A modified fuzzy C-means algorithm for bias field estimation and segmentation of MRI data," *IEEE Trans. Med. Imag.*, vol. 21, no. 3, pp. 193–199, Mar. 2002.
[26] H. Verma, R. K. Agrawal, and N. Kumar, "Improved fuzzy entropy clustering algorithm for MRI brain image segmentation," *Int. J. Imag. Syst. Technol.*, vol. 24, no. 4, pp. 277–283, Dec. 2014.
[27] R. Caruana, "Multitask learning," *Mach. Learn.*, vol. 28, no. 1, pp. 41–75, Jul. 1997.
[28] S. J. Pan and Q. Yang, "A survey on transfer learning," *IEEE Trans. Knowl. Data Eng.*, vol. 22, no. 10, pp. 1345–1359, Oct. 2009.
[29] L. Jacob, J.-P. Vert, and F. R. Bach, "Clustered multi-task learning: A convex formulation," in *Proc. 21st Int. Conf. Neural Inf. Process. Syst.*, Vancouver, BC, Canada, 2008, pp. 745–752.
[30] Q. Gu and J. Zhou, "Learning the shared subspace for multi-task clustering and transductive transfer classification," in *Proc. 9th Int. Conf. Data Mining*, Miami, FL, USA, Dec. 2009, pp. 159–168.
[31] Z. Zhang and J. Zhou, "Multi-task clustering via domain adaptation," *Pattern Recognit.*, vol. 45, no. 1, pp. 465–473, Jan. 2012.
[32] J. Blitzer, R. McDonald, and F. Pereira, "Domain adaptation with structural correspondence learning," in *Proc. Conf. Empirical Methods Natural Lang. Process.*, Sydney, NSW, Australia, 2006, pp. 120–128.
[33] W. Zhong and J. Kwok, "Convex multitask learning with flexible task clusters," in *Proc. 29th Int. Conf. Mach. Learn.*, Edinburgh, Scotland, 2012, pp. 483–490.
[34] Y. Nesterov, "Gradient methods for minimizing composite objective function," *Core Discuss. Papers*, vol. 140, no. 1, pp. 125–161, Sep. 2007.
[35] L. Xu, A. Huang, J. Chen, and E. Chen, "Exploiting task-feature co-clusters in multi-task learning," in *Proc. 29th AAAI Conf. Artif. Intell.*, Austin, TX, USA, 2015, pp. 1931–1937.
[36] T. Evgeniou and M. Pontil, "Regularized multi–task learning," in *Proc. 10th ACM SIGKDD Int. Conf. Knowl. Discovery Data Mining*, Seattle, WA, USA, 2004, pp. 109–117.
[37] T. M. Heskes, "Empirical Bayes for learning to learn," in *Proc. 17th Int. Conf. Mach. Learn.*, Stanford, CA, USA, 2000, pp. 367–374.
[38] L. Liang and V. Cherkassky, "Connection between SVM+ and multi-task learning," in *Proc. IEEE Int. Joint Conf. Neural Netw.*, Hong Kong, Jun. 2008, pp. 2048–2054.
[39] V. Vapnik, *Estimation of Dependences Based on Empirical Data*. New York, NY, USA: Springer, 2006.
[40] J. Zhu, N. Chen, and E. P. Xing, "Infinite latent SVM for classification and multi-task learning," in *Proc. 24th Int. Conf. Neural Inf. Process. Syst.*, Granada, Spain, 2011, pp. 1620–1628.
[41] J. Zhu, N. Chen, and E. P. Xing, "Infinite SVM: A Dirichlet process mixture of large-margin kernel machines," in *Proc. 28th Int. Conf. Mach. Learn.*, Bellevue, WA, USA, 2011, pp. 617–624.
[42] X. He, G. Mourot, D. Maquin, J. Ragot, P. Beauseroy, A. Smolarz, and E. Grall-Maës, "Multi-task learning with one-class SVM," *Neurocomputing*, vol. 133, pp. 416–426, Jun. 2014.
[43] B. Schölkopf, J. C. Platt, J. C. Shawe-Taylor, A. J. Smola, and R. C. Williamson, "Estimating the support of a high-dimensional distribution," *Neural Comput.*, vol. 13, no. 7, pp. 1443–1471, Jul. 2001.
[44] S. Xu, X. An, X. Qiao, and L. Zhu, "Multi-task least-squares support vector machines," *Multimedia Tools Appl.*, vol. 71, no. 2, pp. 699–715, Jul. 2014.
[45] J. A. K. Suykens and J. Vandewalle, "Least squares support vector machine classifiers," *Neural Process. Lett.*, vol. 9, no. 3, pp. 293–300, Jun. 1999.
[46] Y. Li, X. Tian, M. Song, and D. Tao, "Multi-task proximal support vector machine," *Pattern Recognit.*, vol. 48, no. 10, pp. 3249–3257, 2015.
[47] O. L. Mangasarian and E. W. Wild, "Proximal support vector machine classifiers," in *Proc. 7th ACM SIGKDD Int. Conf. Knowl. Discovery Data Mining*, San Francisco, CA, USA, 2001, pp. 77–86.
[48] X. Xie and S. Sun, "Multitask centroid twin support vector machines," *Neurocomputing*, vol. 149, pp. 1085–1091, Feb. 2015.
[49] Jayadeva, R. Khemchandani, and S. Chandra, "Twin support vector machines for pattern classification," *IEEE Trans. Pattern Anal. Mach. Intell.*, vol. 29, no. 5, pp. 905–910, May 2007.
[50] M. T. Hooijmans, O. Dzyubachyk, K. Nehrke, P. Koken, M. J. Versluis, H. E. Kan, and P. Börnert, "Fast multistation water/fat imaging at 3T using DREAM-based RF shimming," *J. Magn. Reson. Imag.*, vol. 42, no. 1, pp. 217–223, Jul. 2015.
[51] H. Zaidi, N. Ojha, M. Morich, J. Griesmer, Z. Hu, P. Maniawski, O. Ratib, D. Izquierdo-Garcia, Z. A. Fayad, and L. Shao, "Design and performance evaluation of a whole-body Ingenuity TF PET–MRI system," *Phys. Med. Biol.*, vol. 56, no. 10, pp. 3091–3106, May 2011.
[52] A. Kalemis, B. M. A. Delattre, and S. Heinzer, "Sequential whole-body PET/MR scanner: Concept, clinical use, and optimisation after two years in the clinic. The manufacturer's perspective," *Magn. Reson. Mater. Phys., Biol. Med.*, vol. 26, no. 1, pp. 5–23, Feb. 2013.
[53] K.-H. Su, L. Hu, C. Stehning, M. Helle, P. Qian, C. L. Thompson, G. C. Pereira, D. W. Jordan, K. A. Herrmann, M. Traughber, R. F. Muzic, Jr., and B. J. Traughber, "Generation of brain pseudo-CTs using an undersampled, single-acquisition UTE-mDixon pulse sequence and unsupervised clustering," *Med. Phys.*, vol. 42, no. 8, pp. 4974–4986, Jul. 2015.

**YIZHANG JIANG** (M'12) received the Ph.D. degree from Jiangnan University, Wuxi, China, in 2015, where he is currently an Associate Professor with the School of Digital Media. He has also been a Research Assistant with the Department of Computing, Hong Kong Polytechnic University, for two years. His research interests include pattern recognition, intelligent computation, and their applications. He is the author or coauthor of more than 50 research articles in international/national journals, including the IEEE Transactions on Fuzzy Systems, the IEEE Transactions on Neural Networks and Learning Systems, the IEEE Transactions on Cybernetics, the *ACM Transactions on Multimedia Computing, Communications, and Applications*, and the *Information Sciences*. He has served as a Reviewer or Co-Reviewer for several international conferences and journals, such as the ICDM, TKDE, TFS, TNNLS, *Pattern Recognition*, the *Neurocomputing*, and the *Neural Computing and Applications*. He has also served as a Lead Guest Editor or Guest Editor for several international journals, such as the *Journal of Ambient Intelligence and Humanized Computing* and the *Journal of Cloud Computing*.

**JIAMIN ZHENG** is currently pursuing the M.S. degree with the School of Digital Media, Jiangnan University, China. Her research areas include machine learning and its applications on medicine.

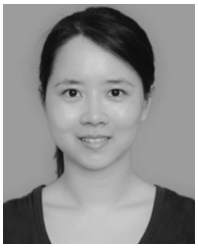

**XIAOQING GU** received the Ph.D. degree from Jiangnan University, Wuxi, China, in 2017. She is currently a Lecturer with the School of Information Science and Engineering, Changzhou University, Changzhou, China. She has published over 20 articles in international/national authoritative journals. Her current research interests include pattern recognition and machine learning.

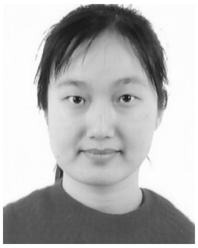

**JING XUE** received the M.D. (Doctor of Medicine) degree from the Department of Nephrology, Nanjing Medical University, Nanjing, China, in 2019, and the M.M. degree from the Department of Nephrology, Nanjing Medical University. She is currently a Doctor with the Affiliated Wuxi People's Hospital of Nanjing Medical University, China. Her research areas include machine learning and its applications on medicine.

**PENGJIANG QIAN** (M'12) received the Ph.D. degree from Jiangnan University, Wuxi, China, in 2011. He is currently a Professor with the School of Digital Media, Jiangnan University, and also with the Case Western Reserve University, Cleveland, OH, USA, as a Research Scholar in medical image processing. His current research interests include data mining, pattern recognition, bioinformatics and their applications, such as analysis and processing for medical imaging, intelligent traffic dispatching, and advanced business intelligence in logistics. He has authored/coauthored over 60 articles in international/national journals and conferences.